Low-temperature thermal relaxation of electrons in one-dimensional nanometer-size structures

S. Das Sarma and V. B. Campos*
Joint Program for Advanced Electronic Materials, Department of Physics, University of Maryland, College Park, Maryland 20742
(Received 28 August 1992; revised manuscript received 29 October 1992)

We calculate the low-temperature power loss due to acoustic-phonon emission via the deformation-potential electron-lattice coupling by warm one-dimensionally confined electrons in GaAs quantum wires. The most spectacular feature of one-dimensional thermal relaxation, arising from the dominance of $2k_F$ scattering at very low temperatures, is an exponential temperature dependence of power loss at the lowest electron temperatures, in contrast to the well-known Bloch-Grüneisen algebraic temperature dependence in higher dimensions. We find that, in contrast to two- and three-dimensional systems, the temperature dependence of the power loss is rather strongly density dependent and remains qualitatively unaffected by electronic screening in one dimension. The magnitude of the one-dimensional power loss is comparable to that in two-dimensional heterostructures except at the lowest temperatures, where the one-dimensional power loss is exponentially suppressed.

One of the early technological motivations for studying one-dimensionally confined electrons in semiconductor quantum wires was the suggestion[1] that at low temperatures, when the Fermi surface is sharply defined, elastic impurity scattering of the carriers will be drastically reduced because energy conservation in one dimension allows only $2k_F$ resistive elastic scattering. In fact, if one takes the one-dimensional model seriously,[2] then within the leading-order random-phase-approximation (RPA) zero-temperature screening becomes logarithmically divergent precisely at $2k_F$, completely suppressing any elastic (resistive) scattering. Of course, in real quantum wires at finite temperatures there will be residual impurity scattering arising from thermal broadening of the Fermi distribution function and from intersubband processes.[3] But, in high-quality modulation-doped semiconductor quantum wire structures, it is probably reasonable to assume that impurity scattering contribution to linear Ohmic resistivity will be small. It is, therefore, of some importance to understand the nonlinear transport properties[4] of semiconductor quantum wires. In particular, thermal relaxation of hot quantum wire carriers at low temperatures (with the carrier temperature slightly higher than the ambient temperature) is controlled by the acoustic phonon emission process. We point out that at ultralow temperatures phonon scattering is also suppressed in one-dimensional systems, leading to exponentially weak hot-electron relaxation at the lowest electron temperatures. In this paper, by considering two different phonon models, we develop a theory for the energy loss rate of warm one-dimensionally confined electrons at an electron temperature T which is slightly above the lattice temperature $T_{\rm lat}$ so that acoustic-phonon emission is the only important dissipative process. In one model, more appropriate when the electron gas is strongly coupled to the substrate lattice, the phonons are chosen to be the usual bulk three-dimensional phonons (referred to as the 3D model). In the other model, more appropriate for free standing quantum wires where the phonon modes are also one-dimensionally confined, both the electrons and the phonons are taken to be one dimensional (the 1D model). Note that the electrons are treated in exactly the same one-dimensional confinement model in both cases. We assume the validity of the electron temperature model throughout, describing the warm-electron gas by a Fermi distribution function at an elevated temperature $T > T_{\rm lat}$. This model is known to be a reasonable model in the steady-state electric field heating situation. We consider only the intrasubband relaxation within the lowest one-dimensional subband, neglecting all effects of higher subbands in our calculation.

The average energy-loss rate via acoustic-phonon scattering can be written as

$$\left\langle \frac{dE}{dt} \right\rangle = \frac{1}{N} \sum_{\mathbf{q}} \hbar\omega_{\mathbf{q}} \frac{dN_q}{dt} , \tag{1}$$

where N is the total number of electrons, $\hbar\omega_{\mathbf{q}}$ is the phonon energy for wave vector $\mathbf{q}$, and dN_q/dt is the rate of change of the phonon distribution function. From Fermi's "golden rule," dN_q/dt is easily calculated to be

$$\frac{dN_q}{dt} = 2\left[\frac{2\pi}{\hbar}\right] \sum_{\mathbf{k}} |M(q)|^2 \delta(E_{\mathbf{k}} + \hbar\omega_{\mathbf{q}} - E_{\mathbf{k}+\mathbf{q}}) \{(N_q+1) f(E_{\mathbf{k}+\mathbf{q}_\parallel})[1-f(E_{\mathbf{k}})] - N_q f(E_{\mathbf{k}})[1-f(E_{\mathbf{k}+\mathbf{q}_\parallel})]\} , \tag{2}$$

where the summation is over the electron wave vector $\mathbf{k}$ and the phonon wave vector $\mathbf{q}=(\mathbf{q}_\parallel,\mathbf{q}_\perp)$ is decomposed into components parallel and perpendicular to the electron wave vector. The matrix element $|M(q)|^2$ is the electron-phonon interaction matrix element via the deformation-potential coupling. The quantities f and E are the electron distribution function and energy, respectively. Putting Eq. (2) in Eq. (1), one obtains the basic

equation for the hot-electron energy-loss rate via phonon emission in any dimension[5,6]—the information about confinement and dimensionality enters through the interaction matrix element $|M(q)|^2$. One can include screening in the calculation by using the appropriately screened deformation-potential interaction matrix element.

It is instructive to write the equation for power loss $P=\langle dE/dt \rangle$, obtained by substituting Eq. (2) in Eq. (1), in a mathematically equivalent form by using the fluctuation-dissipation theorem:

$$P=\left[\frac{1}{N}\right]\sum_{\mathbf{q}}\hbar\omega_{\mathbf{q}}|M(q)|^2[N_T(\omega_{\mathbf{q}})-N_{T_{\rm lat}}(\omega_{\mathbf{q}})] \times \mathrm{Im}\Pi_T(\mathbf{q},\omega_{\mathbf{q}}) , \quad (3)$$

where Π is the electronic polarizability function and $N_{T(T_{\rm lat})}$, as before, is the Bose factor at the temperature $T(T_{\rm lat})$. In Eq. (3), confinement and dimensionality show up in calculating $\Pi_T(\mathbf{q},\omega_{\mathbf{q}})$ and $|M(q)|^2$ (as well as the phonon frequency $\omega_{\mathbf{q}}$). This expression for the hot-electron power loss, which is formally independent of dimensions and the phonon modes involved, has been extensively used in the literature in calculating the longitudinal-optical phonon emission rate.[7,8]

We have used the deformation-potential approximation for the electron-acoustic-phonon coupling matrix element:

$$|M(q)|^2=\left[\frac{Z^2\hbar q}{2\rho u}\right]\{I(q_y)I(q_z)\} , \quad (4)$$

where the first term in the square brackets is the usual deformation-potential coupling with Z the deformation-potential coupling constant, ρ and u being, respectively, the ionic mass density and the longitudinal sound velocity. The second term within the curly brackets of Eq. (4) is the quantum-mechanical form factor arising from confinement in y and z directions. We calculate the quantum form factors in the infinite square potential-well confinement model[2,7] with the same confinement width in the y and z directions. We assume the one-dimensional limit in our calculation, taking only the lowest subband for y and z motion to be occupied by the electrons, and consider intrasubband electron-phonon scattering processes only. Our calculation is for GaAs quantum wires, where the one-dimensional limit of a strict one subband occupancy has recently been achieved experimentally.[9]

In the rest of this paper we present our numerical results for the calculated hot-electron power loss via acoustic phonon emission in GaAs quantum wires (taking $Z=10$ eV) as a function of electron and lattice temperatures and carrier density. The electron wave vector $\mathbf{k}\equiv k_x$ is one dimensional in all our equations. For the 3D model, we take $\mathbf{q}$ to be the three-dimensional phonon wave vector and $I(q_y),I(q_z)$ are calculated corresponding to infinite square well confinement defined by the widths $L_y=L_z=100$ Å. For the 1D model, the phonon wave vector $\mathbf{q}\equiv q_x$ is one dimensional as well and, because we are interested in qualitative behavior, we make the additional simplifying approximation of choosing $I(q_y)=I(q_z)=1$ without worrying about the details of the phonon confinement. We also assume that the form of the deformation-potential coupling matrix element, given by Eq. (4), is the same for the 3D and the 1D model and that the acoustic phonon dispersion is of the same linear form, $\omega_{\mathbf{q}}=u|\mathbf{q}|$, in both cases. The calculation of power loss then involves carrying out a two-dimensional integration in the right-hand side of Eq. (3)—one to obtain Π_T at finite temperatures and the other over the magnitude q of the phonon wave vector to do the sum over $\mathbf{q}$. [The form factors $I(q_y)$ and $I(q_z)$ are also two-dimensional integrals making the total integral for P a four-dimensional one for the 3D model.] The integral over the wave vector q is cut off at a Debye wave vector q_D to eliminate the artificial ultraviolet divergence arising from the use of an electron gas model. Screening is included in some of our calculations within the static random-phase approximation by using the reducible (i.e., screened) one-dimensional electron polarizability function[10] for Π.

The most spectacular feature of one-dimensional thermal relaxation is the ultralow-temperature ($k_BT\ll E_F$) behavior of the calculated power loss which is exponentially weak in contrast to the well-known Bloch-Grüneisen algebraic temperature dependence[5] in two- and three-dimensional systems. This exponential behavior follows from the peculiar nature of the one-dimensional Fermi surface which at low temperatures ($k_BT\ll E_F$) is simply two points at $k=\pm k_F$ with all the states in between completely filled and those outside (i.e., with $|k|>k_F$) empty. The only possible intrasubband relaxation mechanism at this ultralow ($k_BT\ll E_F$) temperature is provided by the $2k_F$ scattering as an acoustic phonon of wave vector $2k_F$ is emitted. At low temperatures, the emission of such a phonon is obviously exponentially suppressed leading to the temperature dependence (for $k_BT\ll E_F$)

$$P\propto e^{-\hbar(2uk_F)/k_BT}$$

for the electron energy loss (with $T_{\rm lat}=0$), where $2uk_F=\omega_{2k_F}$ is the frequency of the emitted $2k_F$ acoustic phonon. The same result follows easily from Eqs. (2) or (3) as well.

In Fig. 1 we show our numerically calculated low-temperature power loss as a function of the electron temperature T (with $T_{\rm lat}=0$) for various 1D electron densities in both the 3D and the 1D model. The exponential drop in the power loss is obvious in the low-temperature regime of Fig. 1. Note that with decreasing electron density, the exponential regime gets shifted to lower electron temperatures because the condition $k_BT\ll E_F$ is satisfied at lower temperatures for lower electron densities. Note also that the inclusion of screening decreases the power loss slightly without affecting its qualitative temperature dependence. This spectacular exponential suppression of the low-temperature one-dimensional intrasubband thermal relaxation rate is the most important qualitative result of this work.

At electron temperatures which are not too low compared with the Fermi temperature ($T \gtrsim T_F$ or higher, where $T_F = E_F/k_B$ is the Fermi temperature), but still low compared with the characteristic phonon energies (i.e., for $T_F < T \ll \theta_D$, where θ_D is the Debye temperature), the power loss (for $T_{\text{lat}} = 0$) is characterized by a "Bloch-Grüneisen" type algebraic temperature dependence, $P \sim T^n$, where the exponent n can be estimated from Eq. (3) [or Eq. (2)] by the usual power-counting technique. The crossover from the exponential temperature dependence at ultralow temperatures ($T \ll T_F$) to the algebraic temperature dependence at intermediate temperatures ($T_F \lesssim T \ll \theta_D$) in the calculated power loss can be seen in Fig. 1 essentially around $T \sim 1$ K temperature region. We explore this intermediate-temperature region in Figs. 2–4. In the results discussed below (Figs. 2–5) we do not further discuss the exponential ultralow-temperature ($T \ll 1$ K) regime and concentrate on the intermediate-temperature regime instead ($T \sim 1$–10 K). The exponential temperature dependence around $T \sim 0$ K

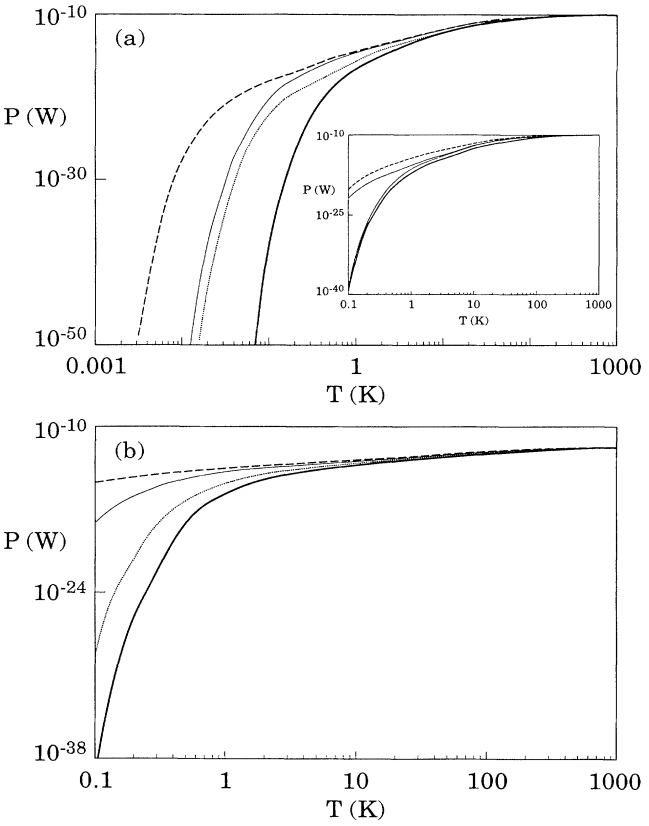

FIG. 1. Shows the calculated one-dimensional power loss, P, in watts as a function of the electron temperature, T, in kelvin (for $T_{\text{lat}} = 0$ K) on a log-log plot for (a) the 3D and (b) the 1D phonon models. In the inset of (a) statistically screened 3D phonon results for two densities are shown (all the other results are unscreened). Different curves indicate different 1D electron densities: $N = 0.1 \times 10^5$ (dashed curve), 1.0×10^5 (thin solid curve), 3.0×10^5 (dotted curve), and 5.0×10^5 cm (thick solid curve) in (a) and (b) whereas in the inset of (a) the dashed and the thin solid lines represent, respectively, the unscreened and the screened $N = 1.0 \times 10^5$ cm^{-1} case, and the dotted and the thick solid lines represent, respectively, the unscreened and the screened $N = 5.0 \times 10^5$ cm^{-1} case. The low-temperature exponential behavior and the intermediate-temperature algebraic behavior can both be seen in these results. ($L_y = L_z = 100$ Å.)

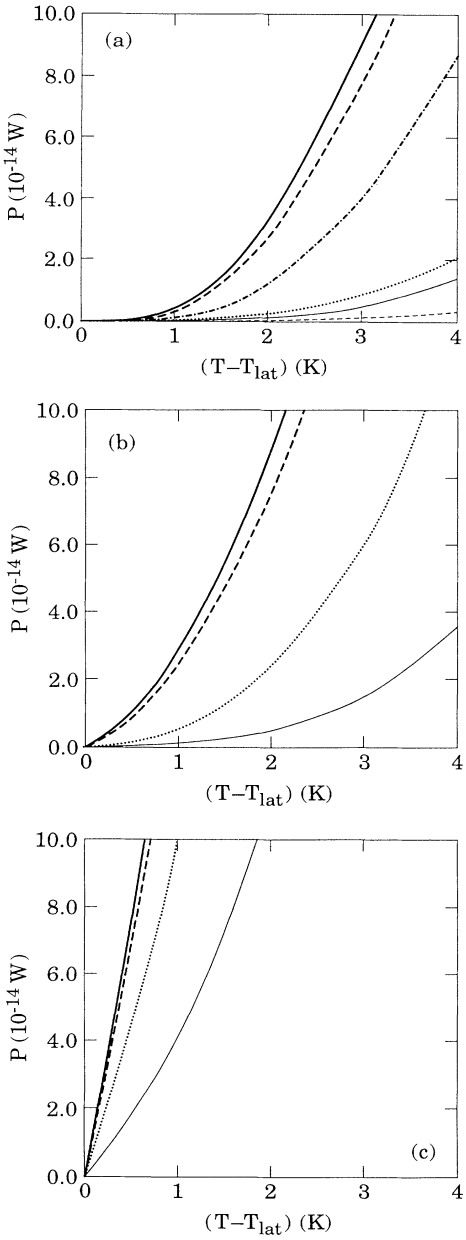

FIG. 2. Shows the calculated power loss P (per electron) as a function of the electron (T) and the lattice (T_{lat}) temperature difference for the 3D model and for several carrier densities $N = 0.1 \times 10^5$ (thick solid curve), 1.0×10^5 (dashed curve), 5.0×10^5 cm (thin solid curve), and for $T_{\text{lat}} = 0$ K (a), 1 K (b), 5 K (c). In Fig. 1(a) the screened results are also shown for $N = 0.1 \times 10^5$ (dot-dashed curve) and 1.0×10^5 cm (dotted curve) densities. Only the intermediate-temperature regime can be seen in these linear plots. ($L_y = L_z = 100$ Å.)

for the power loss is not manifest in the linear temperature scale of Figs. 2 and 3.

In Fig. 2 we show, for the 3D model, the calculated power loss as a function of the electron and lattice temperature difference $(T-T_{\rm lat})$ in the intermediate-temperature range for a number of different carrier densities and for $T_{\rm lat}=0$ [Fig. 2(a)], 1 K [2(b)], and 5 K [2(c)]. In Fig. 2(a) we also depict the screened results for the sake of comparison. In Fig. 3 we show P as a function of $(T-T_{\rm lat})$ for the 1D model. The calculated power loss for 1D and 3D models are comparable (in the 10^{-14} W range for $T-T_{\rm lat}$ around a few K) in magnitudes and it is, in fact, similar[5] to the hot-electron energy loss rate in two-dimensional heterostructures for the same range of parameters. But the temperature dependence of P is different in the two models with the temperature exponent of P being much higher for the 3D model than for the 1D model [compare Fig. 2(a) with Fig. 2(b)]. This is actually expected on the basis of simple dimensional arguments which indicate that the 3D model should have an exponent n (i.e., $P\sim T^n$ for $T_{\rm lat}=0$) which is higher than that for the 1D model by 2. One interesting feature, which distinguishes one-dimensional hot-electron power loss from higher-dimensional results,[5] is that screening [see Fig. 2(a)] does not change the qualitative low-temperature behavior of the calculated power loss, i.e., the exponent n is unaffected by screening in one dimension (in contrast to higher dimensions). This behavior follows naturally from the weak wave-vector dependence of one-dimensional screening.[2,10]

In Fig. 4 we show the carrier density dependence of the calculated power loss for the 3D and the 1D model. The power loss is more than an order of magnitude larger in the 3D model compared to the 1D model at higher electron temperatures because of the much stronger tempera-

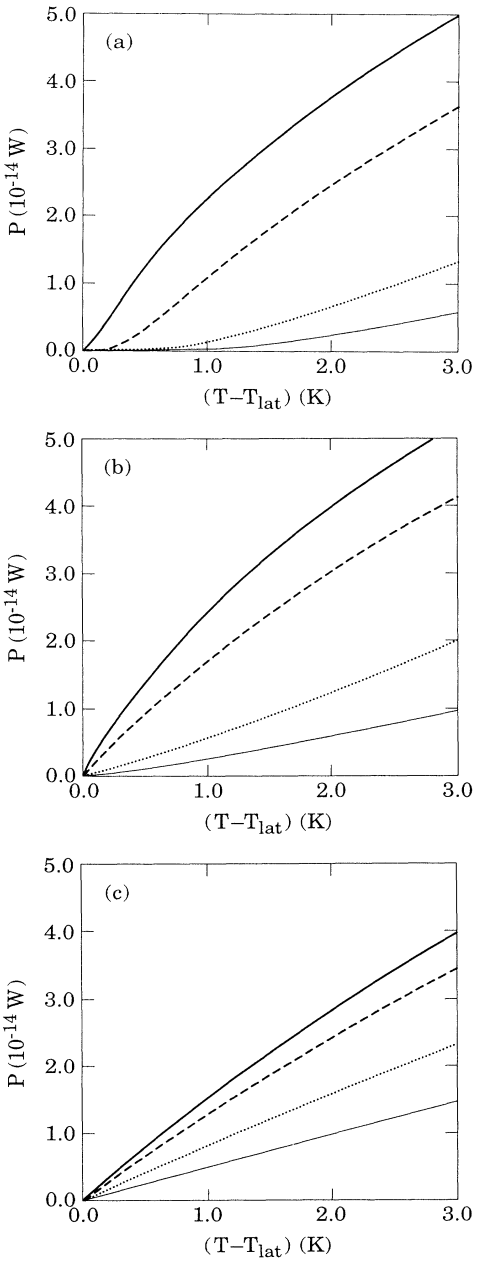

FIG. 3. The same as in Fig. 2 for the 1D model (without any screened results).

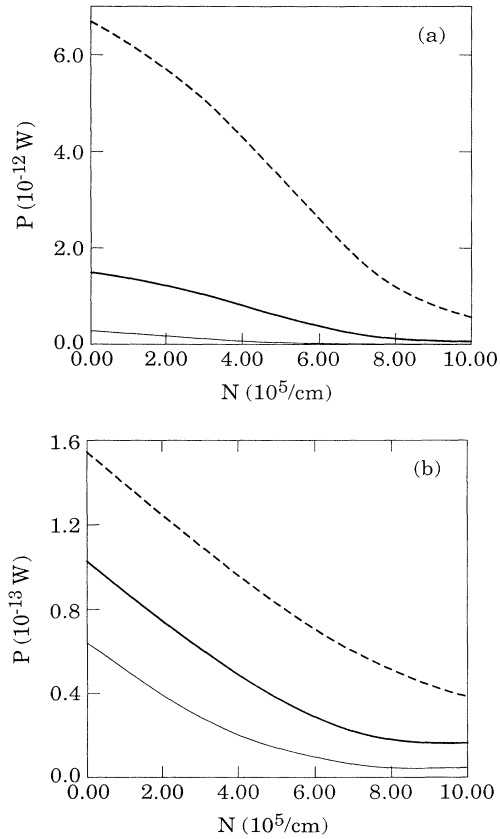

FIG. 4. Shows the carrier density (N) dependence of P for $T=5$ K (thin solid line), 10 K (thick solid line), 20 K (dashed line), and for (a) the 3D and (b) the 1D model. ($T_{\rm lat}=1$ K, $L_y=L_z=100$ Å.)

ture dependence of the relaxation rate in the 3D model. Also, the density dependence of the calculated power loss is strong in both the models, in sharp contrast to two-dimensional heterostructures,[5] where the low-temperature power loss due to acoustic phonon emission is essentially density independent. The strong density dependence of Fig. 4 arises from the rather low degeneracy temperatures (Fermi temperatures T_F) in the achievable carrier density range ($\sim 10^5$ cm^{-1}) in one-dimensional systems. In fact, for high densities or for low electron temperatures, the one-dimensional result is also essentially density independent in qualitative similarity to higher-dimensional[5] acoustic phonon emission mediated cooling results. The large ($\sim$ a factor of 10 for higher values of T) difference in the power loss between 3D and 1D results is also real because the 1D model, being severely restrictive in phase space, allows substantially less cooling. This difference, as well as the qualitative difference in the temperature dependence of P at low T, should be sufficient to differentiate between the models when experimental data become available. We believe that the actual results should lie somewhere between the two models (our two models being two extreme simplifications), perhaps closer to the 3D results than the 1D ones. For truly free standing quantum wires, the 1D model may be more suitable.

Finally, in Fig. 5 we show our calculated one-dimensional power loss via acoustic phonon emission for the two models over a wider temperature range, comparing it with the corresponding bulk (i.e., 3D) LO-phonon emission mediated power loss.[7] For $(T-T_{\rm lat})>40-50$ K, the calculated power loss is exponentially greater via LO-phonon emission, and acoustic phonon processes are unimportant. But below 30 K power loss via acoustic phonon emission is the dominant process, because LO-phonon emission is exponentially suppressed.

We now briefly consider the asymptotic temperature dependence of the power loss as implied by Eqs. (1)–(4) in the intermediate-temperature range ($T_F \lesssim T \ll \theta_D$). For $T_{\rm lat}=0$ (and without any screening) it is straightforward

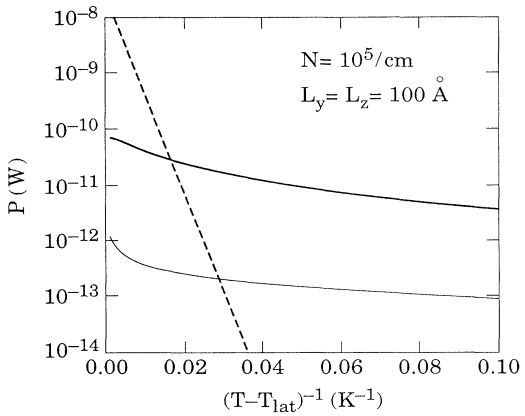

FIG. 5. Shows P as a function of $(T-T_{\rm lat})^{-1}$ on a semilogarithmic plot for the 3D (solid line), 1D (thin solid line), and the LO-phonon emission (dashed line) models.

to extract the intermediate-temperature ($k_B T \ll \hbar\omega_q \sim \hbar\omega_D$) behavior of the power loss by a simple power counting. One gets $P\sim T^n$ with $n=5$ for the 3D model and $n=3$ for the 1D model. At very low T, as emphasized earlier, the temperature dependence of the power loss is exponential, arising from the peculiar nature of the one-dimensional Fermi surface which makes the $2k_F$ scattering the only allowed relaxation process—but, the crossover occurs at a very low temperature where the power loss is small ($\lesssim 10^{-15}$ W). Our numerical results shown in Figs. 2–4 are consistent with these intermediate-temperature Bloch-Grüneisen exponents ($n=3$ and 5 for the 1D and the 3D models, respectively). One can see from a comparison of Figs. 2 and 3 that the numerical value of intermediate temperature n for the 3D model (Fig. 2) is substantially larger than that for the 1D model (Fig. 3). For large T, the Bose factor in Eq. (3) dominates and gives $P\sim T$ (i.e., $n=1$)—this, however, is not a physically meaningful result because in the high-T ($>30-40$ K) regime, LO-phonon emission is the dominant dissipative process. We should also mention that for $T_{\rm lat}\neq 0$, the power loss is linear in $(T-T_{\rm lat})=\Delta T$ for small values of ΔT which is consistent with our numerical results of Figs. 2 and 3.

It is well known[5] that in two-dimensional heterostructures the bare exponent n changes drastically when screening is included in the theory. A curious aspect of one-dimensional screening behavior is that the exponent n remains unaffected by screening. This can be seen in Fig. 1(a) where screening lowers the quantitative magnitude of the power loss, but does not change the low-T exponent. It is easy to show that one-dimensional RPA screening[10] at long wavelengths, as given by the static dielectric function, goes as $\varepsilon(q)\simeq 1+A\,|\ln(qa)|$ where $A^{-1}=\hbar^2\varepsilon_{\rm lat}\pi k_F/4me^2$ is a constant. Inclusion of screening in Eqs. (1)–(4), therefore, would only introduce logarithmic temperature corrections to the bare result, without affecting the exponent n.

We emphasize that there is really no true Bloch-Grüneisen regime in one-dimensional systems where the low-temperature power loss via acoustic phonon emission has an exponential electron temperature dependence. The asymptotic low-temperature dependence of the power loss is always exponentially activated in temperature due to the peculiar dominance of $2k_F$ scattering in one dimension. The very-high-temperature behavior is linear in temperature. There is an intermediate-temperature regime (1–10 K), where the power loss simulates an algebraic temperature dependence, $P\sim T^n$, with $n\sim 3-6$ depending on the phonon model. But this is a crossover regime and *not* an asymptotic temperature dependence in contrast to the usual Bloch-Grüneisen behavior in higher dimensions. There are corrections to the exponent n in this intermediate crossover temperature regime, arising from the temperature dependence of the electron Fermi factors in Eq. (2) [or, equivalently, from the temperature dependence of ImΠ in Eq. (3)], which are, of course, exactly included in our numerical results but are missed by the simple counting arguments leading to $n=3$ or 5 in one dimension.

We conclude by mentioning that in two-dimensional

heterostructures the exact value of the deformation-potential coupling constant Z has been a controversial[5] issue with $Z=7-14$ eV being used in the literature for GaAs. We have used $Z=10$ eV in all our calculations, but, of course, one can change Z by simply scaling our numerical results by Z^2. It will be interesting to see whether the experimental results for power loss in one-dimensional quantum wires will also require an enhanced value of Z as is the case for heterostructures. It should be pointed out that our single-subband model of a symmetric square cross-section quantum wire with infinite potential barriers is not a very realistic one and may need to be improved for comparison with experimental results. A comparison with experimental results, when they become available, may also require a substantial extension of our theory by including, in general, the effects of higher subbands and, in particular, the effect of intersubband scattering on the relaxation rate. Intersubband scattering will modify some of the purely one-dimensional peculiarities of our results—in particular, the exponential suppression of power loss at low temperatures should disappear if intersubband scattering is significant.

This work was supported by the U.S. ARO and the U.S. ONR.

---

*On leave from Universidade Federal de São Carlos, Brazil.

[1]H. Sakaki, Jpn. J. Appl. Phys. **19**, L735 (1980).
[2]S. Das Sarma and W. Y. Lai, Phys. Rev. B **32**, 1401 (1985).
[3]S. Das Sarma and X. C. Xie, Phys. Rev. B **35**, 9875 (1987).
[4]S. Briggs and J. P. Leburton, Phys. Rev. B **43**, 4785 (1991); **38**, 8163 (1988).
[5]T. Kawamura *et al.*, Phys. Rev. B **42**, 5407 (1990); J. Manion *et al.*, *ibid.* **35**, 9203 (1987); K. Hirakawa and H. Sakaki, Appl. Phys. Lett. **49**, 889 (1986); P. J. Price, J. Appl. Phys. **53**, 6863 (1982).
[6]P. B. Allen, Phys. Rev. Lett. **59**, 1460 (1987).
[7]V. B. Campos and S. Das Sarma, Phys. Rev. B **45**, 3898 (1992).
[8]S. Das Sarma, J. K. Jain, and R. Jalabert, Phys. Rev. B **41**, 3561 (1990).
[9]A. R. Goni *et al.*, Phys. Rev. Lett. **67**, 3298 (1991); A. S. Plaut *et al.*, *ibid.* **67**, 1642 (1991).
[10]Q. P. Li and S. Das Sarma, Phys. Rev. B **43**, 11 768 (1991).